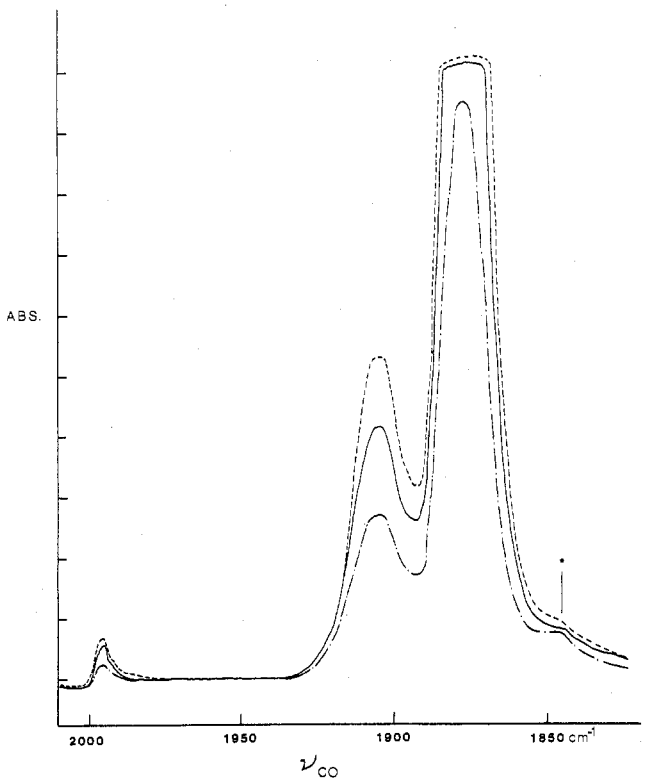

Figure 1. Infrared spectra in the ν(CO) region of [PPN][$HFe(CO)_4$] in tetrahydrofuran: —, prepared from $Na^{16}OH$; - - -, prepared from $Na^{18}OH$; –·–, prepared from $Na^{18}OH$ under phase-transfer conditions. Peak marked by asterisk corresponds to a mono-$C^{18}O$-labeled $HFe(CO)_4^-$ species (see ref 12 for the analogous ^{13}CO assignment since both $C^{18}O$ and ^{13}CO substitutions result in essentially identical ν(CO) shifts).

$HFe(CO)_4^-$ (~10%). Even under these mildly basic conditions oxygen exchange was only barely discernible (<2% oxygen-18 enrichment in $HFe(CO)_4^-$ (see Figure 1)).[14]

The consequences of these investigations clearly point out the propensity of $Fe(CO)_5$ to proceed to the anionic carbonyl hydride species $HFe(CO)_4^-$ as opposed to undergoing oxygen exchange under the conditions of the water–gas shift catalysis. This would suggest that in this catalytic system as in its $Ru_3(CO)_{12}$ analogue,[2] reductive elimination of H_2 may be the rate-determining step in hydrogen production following initial attack of ^-OH at the carbon center in $Fe(CO)_5$.

Consistent with observations made on other metal carbonyl derivatives, substitution of CO by phosphine ligands in $Fe(CO)_5$ retards metal hydride formation.[10]

Acknowledgment. Partial financial support from the National Science Foundation through Grant CHE 78-01758 for this project is greatly appreciated.

Registry No. [PPN][$HFe(CO)_4$], 56791-54-9; $Fe(CO)_5$, 13463-40-6; NaOH, 1310-73-2.

References and Notes

(1) Kang, H. C.; Mauldin, C. H.; Cole, T.; Sleigeir, W.; Cann, K.; Pettit, R. *J. Am. Chem. Soc.* **1977**, *99*, 8323.
(2) Ford, P. C.; Rinker, R. G.; Ungermann, C.; Laine, R. M.; Landis, V.; Moya, S. A. *J. Am. Chem. Soc.* **1978**, *100*, 4595.
(3) King, R. B.; Frazier, C. C.; Hanes, R. M.; King, A. D., Jr. *J. Am. Chem. Soc.* **1978**, *100*, 2925.
(4) Species **2** is known to be a catalyst for olefin isomerization and hydrogenation.[5]
(5) (a) Sternberg, H. W.; Markby, R.; Wender, I. *J. Am. Chem. Soc.* **1957**, *79*, 6116. (b) Schroeder, M. A.; Wrighton, M. S. *Ibid.* **1976**, *98*, 551.
(6) Muetterties, E. L. *Inorg. Chem.* **1965**, *4*, 1841.
(7) Darensbourg, D. J.; Drew, D. *J. Am. Chem. Soc.* **1976**, *98*, 275.
(8) Darensbourg, D. J.; Froelich, J. A. *J. Am. Chem. Soc.* **1977**, *99*, 4726.
(9) Darensbourg, D. J.; Froelich, J. A. *J. Am. Chem. Soc.* **1977**, *99*, 5940.
(10) Darensbourg, D. J.; Froelich, J. A. *J. Am. Chem. Soc.* **1978**, *100*, 338.
(11) Darensbourg, D. J.; Froelich, J. A. *Inorg. Chem.* **1978**, *17*, 3300.
(12) Darensbourg, M. Y.; Darensbourg, D. J.; Barros, H. L. C. *Inorg. Chem.* **1978**, *17*, 297.
(13) Pearson, R. G. "Hard and Soft Acids and Bases"; Dowden, Hutchinson, and Ross: Stroudsburg, PA, 1973.
(14) It would nonetheless be anticipated that as the reaction proceeds further, more highly enriched $HFe(CO)_4^-$ would be formed.

Contribution from the Lash Miller Chemical Laboratories and Erindale College, University of Toronto, Toronto, Ontario, Canada

The Matrix Optical Spectra of Sodium Molecules Containing from Two to Four Atoms

Geoffrey A. Ozin* and Helmut Huber

Received December 4, 1978

A thorough appreciation of small-particle chemistry and physics demands a fundamental knowledge of the size dependence of the electronic, bonding, and structural properties of metallic clusters, especially their convergence behavior toward the bulk metal.[1] Activity–selectivity patterns of high-dispersion metallic catalysts, for example, are understood to be electronic and/or geometric in origin and in principle the metallic substrate and its chemisorption characteristics can be *theoretically modeled* by finite naked clusters M_n and these clusters interacting with ligands, M_nL.[2] Particularly important directions here involve the establishment of appropriate boundary conditions for localized bonding discussions of metal–surface chemistry.[3] Recent *experimental realizations* of model "ligand-free" cluster systems can be seen, for example, in the optical ($Cr_{2,3}$,[4] $Mo_{2,3}$,[4] $Ni_{2,3}$,[5] $Cu_{2,3,4}$,[6] $Ag_{2,3,4,5,6}$,[7] Cr_2Mo,[4] $CrMo_2$[4]), Mössbauer (FeCo;[8a] FeNi;[8a] FeCu;[8a] $Sn_{2,3,4}$;[9] FeMn, Fe_2Mn, $FeMn_2$;[8b] $Fe_{2,3}$[10]), Raman ($Ag_{2,3}$,[11] Mg_2[12]), resonance Raman (Ca_2[13]), fluorescence (Sn_2,[14] Pb_2,[15] $Ag_{2,3}$[16]), and ESR (MgAg,[17] Na_3,[18] Ag_3[19]) spectral studies of a wide range of unimetallic and bimetallic molecules. With the evolution of such unique sets of spectroscopic data concerning few-atom clusters, one can appreciate the necessity for complementary, high-quality, semiempirical,[1,3] and first-principles molecular orbital cluster calculations.[3,20]

In view of the supersonic nozzle beam generation[21a] and laser photoionization mass spectroscopic detection of sodium clusters containing as many as 13 atoms[21b] (which has led to the longest known series of reliable metal cluster ionization potentials), the preparation of gaseous lithium clusters containing up to 15 atoms by evaporation of lithium metal in a high pressure of an inert gas,[22] the ESR detection of matrix entrapped Na_3,[18] the ab initio CI calculations for Na_3[23] as well as numerous other electronic structure calculations of small clusters of alkali metal atoms,[18] and our current interest in group 1A/1B bimetallic cluster systems[24] (the latter, we believe, representing a new synthetic pathway to group 1B cluster anions), we thought it worthwhile to establish the metal concentration and substrate dependence of sodium atom/inert gas condensation–aggregation processes. By employing ultraviolet–visible absorption spectroscopic monitoring of the molecular sodium aggregates so generated, we have managed to tentatively assign some of the optical excitation energies associated with $Na_{2,3,4}$. Such observations should prove to be of considerable worth in the evaluation of future IR/Raman/fluorescence/ESR/two-photon-ionization spectroscopic measurements of Na_n clusters, as well as providing stringent guidelines for assessing the reliability of various metal cluster computational techniques.

0020-1669/79/1318-1402$01.00/0

Experimental Section

In all of the experiments to be described, sodium metal was vaporized at low pressures from a stainless steel Knudsen cell (120–200 °C) and deposited in an almost purely monoatomic form (≤99%) with Kr and Xe matrix gases onto a NaCl optical window cooled to 10–12 K, by using a vacuum furnace, quartz crystal microbalance, and Displex closed-cycle helium refrigeration assembly, the details of which have been previously described.[25] The temperature of the Knudsen cell (orifice diameter 0.5 mm) was monitored by a copper–constantan thermocouple, spot welded close to the orifice of the cell. Absolute deposition rates of sodium vapor into the matrix are not expected to be meaningful in this study, owing to an apparently low sticking coefficient of sodium to our in situ crystal mass monitor, although relative sodium/matrix ratios between different runs are expected to be reliable. We estimate that by this method our matrix ratios could be in error by as much as an order of magnitude and so the quantitative nature of these experiments, vis-a-vis the utilization of a kinetic analysis of the matrix deposition process[42] for determining cluster nuclearity, is open to criticism. However, as only relative $[Na_n]/[Na]$ absorbances are pertinent to the kinetic analysis (below 1% total metal),[42] the growth–decay behavior of the observed sodium cluster lines can be used as a reasonable guide toward establishing cluster nuclearity. Such metal/matrix "cryotitrations", when taken in conjunction with time–temperature profiles of corresponding bulk annealing experiments *as well as photoaggregation behavior*, enable one to distinguish different cluster species in the matrix, to unravel band overlap complications and to arrive at reasonable conclusions concerning cluster nuclearity in the few-atom regime. Optical spectra were recorded on a standard Varian Techtron spectrophotometer in the range 200–900 nm.

Results and Discussion

After mercury, sodium represents a milestone in matrix isolation research in being the second atomic system to be immobilized in a low-temperature support and observed by optical spectroscopy.[26] Since then, matrix entrapped atomic sodium has been of enormous value for understanding a wide variety of spectroscopic phenomena and for generating a plethora of novel chemical syntheses.[27–35]

Despite the intensive interest in sodium atom matrix and macroscale cryochemical reactions, surprisingly little is actually known experimentally about the matrix aggregation properties of atomic sodium itself or about the electronic, geometrical, and bonding properties of small sodium clusters, aside from a matrix ESR study of Na_3,[18] a brief mention of the clustering phenomenon in studies of the 3s excitation of Na atoms entrapped in xenon[36] and benzene[37] matrices, and an unrelated $Na/O_2/Ar$ study of $Na^+(O_2^-)$[38] in which Na_n aggregate absorptions were noted but analysis of these cluster absorptions was not undertaken.

We began our sodium atom matrix aggregation experiments by checking some of the observations of previous workers[26,27] who had examined sodium atom/inert gas cocondensations. Like others,[26,27] we detected the now classic *blue* and *red* triplet absorptions of the $^2S_{1/2} \rightarrow {}^2P_{1/2,3/2}$ sodium atomic resonance transitions in Kr and Xe matrices (see, for example, Figures 1–6) with deposition, annealing, isolation efficiency and substrate behavior in line with earlier observations.[26,27,29,40,41]

A series of Na atom concentration experiments at 10–12 K in Kr and Xe, at matrix ratios in the range $1/10^4$ to $1/10^2$ (as much as an order of magnitude error is to be expected in these ratios—see Experimental Section), clearly revealed a group of new absorptions to the red and blue of the atomic sodium $^2S_{1/2} \rightarrow {}^2P_{1/2,3/2}$ resonance absorptions (a typical series being shown in Figures 1 and 2) which can clearly be identified with sodium aggregates. The relative intensity behavior of these new absorptions on deposition and after temperature-programmed annealing pointed to the existence of at least *three* distinct sodium cluster arrays under the concentration conditions employed in these experiments[42] (see Tables I and II). The onset of cluster formation can be seen, for example, in $Na/Xe \simeq 1/10^4$ matrices by the initial appearance of two

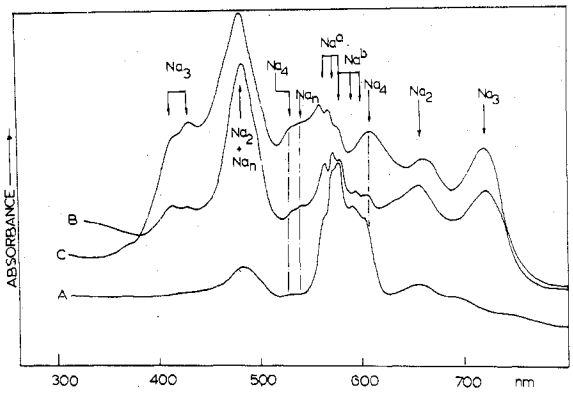

Figure 1. A typical sodium atom–krypton matrix concentration study at 10–12 K [(A) $Na/Kr \simeq 1/10^4$, (B) $Na/Kr \simeq 1/10^3$, (C) $Na/Kr \simeq 1/10^2$] showing the growth–decay behavior of $Na_{1,2,3,4}$. Sodium atom blue and red sites are labeled Na^a and Na^b, respectively (see text and Table II). See Experimental Section for error brackets in these concentration ratios.

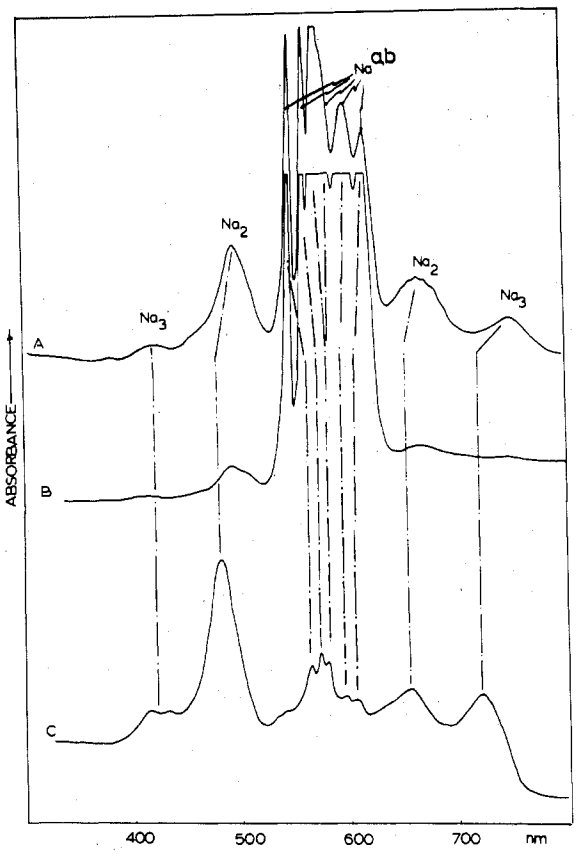

Figure 2. A typical sodium atom–xenon matrix concentration study at 10–12 K [(A) $Na/Xe \simeq 1/10^3$, (B) $Na/Xe \simeq 1/10^4$] showing the growth–decay behavior of $Na_{1,2,3}$ and, for comparison purposes, (C) $Na/Kr \simeq 1/10^3$ showing the correlation with respective $Na_{1,2,3}$ cluster absorptions.

broad absorptions at 494 and 653 nm (Figure 2) which correlate reasonably well with the maximum of the Franck–Condon distributions assigned to the $^1\Sigma_g^+ \rightarrow {}^1\Sigma_u^+$ (X → A) and $^1\Sigma_g^+ \rightarrow {}^1\Pi_u$ (X → B) electronic excitations observed for gas-phase Na_2[43] (apart from small gas-to-matrix phase shifts of the order of 2–20 nm, respectively). On further increase of the sodium atom concentration and hence the opportunity to achieve the trinuclear stage of cluster agglomeration ($Na/Xe \rightarrow 1/10^3$, Figure 2), a second group of new absorptions can be discerned at 750, 420, and 406 nm which straddle both the Na and Na_2 absorptions and can be tentatively associated with the three-atom cluster Na_3, pre-

Table I. Optical Spectral Assignments (nm) for $Na_{1,2,3}$ from Sodium Atom Concentration and Bulk Annealing Experiments in Xenon Matrices

Na	Na_2	Na_3
		750[e]
	653[c,e]	
616, 598, 582 [b,e]		
572, 561, 548 [a,e]		
	494[d,e]	
		420, 406 [e]

[a] Thermally robust sodium atom blue site; can be photoselectively converted into sodium atom red site by using 570-nm narrow-band band excitation. [b] Thermally labile sodium atom red site; rapid bulk diffusion and aggregation in Xe matrices at 20–25 K to $Na_{2,3}$ (Figure 3); can be photoselectively converted into sodium atom blue site by using 598-nm narrow-band excitation. [c] Shows partially resolved vibrational fine structure with average spacing 125–140 cm^{-1} (cf. 118 cm^{-1} for the $X \rightarrow A$ transition for gaseous Na_2). [d] Displays suspected site splitting at 490 nm. [e] 337-nm narrow band excitation causes photobleaching of $Na_{1,2,3}$ absorptions, the clusters decaying at *faster rates* than the atomic species. However, new absorptions, ascribable to either Na_n^+ or Na_n^-, were not observed in the 200–900-nm range. Further Na_2 photokinetic and emission optical matrix experiments will, however, be required to distinguish such a photoionization channel from an alternative Na_2 photofragmentation pathway ($X \rightarrow C$, $^1\Sigma_g^+ \rightarrow {}^1\Sigma_u^+$, 340 nm for gaseous Na_2[43]) with subsequent sodium atom photoinduced diffusion and aggregation to higher Na_n clusters, i.e., Na_2 (337 nm, $h\nu$) $\rightarrow 2Na^\dagger$; $Na^\dagger + Na_n \rightarrow Na_{n+1}$ etc. (see, for example, Cu_2, Ag_2 matrix photofragmentation–photoaggregation processes described in ref 6b) where $Na^\dagger$ represents a photomobile sodium atom.

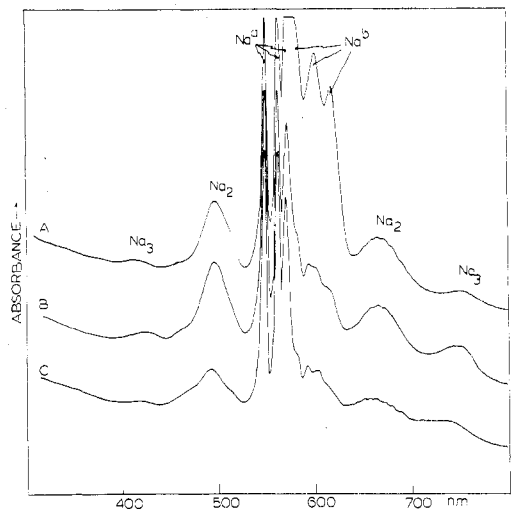

Figure 3. A typical bulk annealing experiment for a $Na_{1,2,3}$/Xe matrix [(A) Na/Xe $\simeq 1/10^3$ deposited at 10–12 K, (B)–(C) after annealing at 20 and 30 K (each for 5 min) and recooling to 10–12 K (cooling time roughly 30–60 s) for spectral recording] showing (i) the thermal lability of the Na^b site and (ii) initial growth of Na_2 and Na_3 up to 20–25 K, followed by decay at 30 K. The thermally robust Na^a site begins to diffuse around 30–40 K.

sumably one and the same species as previously detected by ESR spectroscopy.[18] In this same vein, but working in Na/Kr matrices (Figure 1), it is possible to generate substantial concentrations of $Na_{1,2,3}$ differing only by small, matrix-induced frequency shifts (Table II) from their counterpart absorptions in solid Xe. Under still higher concentration conditions (e.g., Na/Kr $\simeq 1/10^3$ to $1/10^2$ (Figure 1)), one can pinpoint at least two new cluster absorptions around 612 and 530 nm, with a suspected overlap of a third cluster band

Table II. Optical Spectral Assignments (nm) of $Na_{1,2,3,4}$ from Sodium Atom Concentration, Bulk Annealing, and Photoaggregation Experiments in Krypton Matrices

Na^g	Na_2	Na_3	Na_4
		718–730[e]	
			698[f]
	654/660[e]		
			608/615[e]
600, 590, 574 [b]			
574, 566, 558 [a,c]			
			535, 525 [d]
	476–483[e,h]		
		426, 405	

[a] Thermally robust sodium atom blue site (see Figure 1); can be photoselectively converted into sodium atom red site using narrow-band 560-nm excitation under dilute conditions. [b] Thermally labile sodium atom red site; can be photoselectively converted into sodium atom blue site using narrow-band 590-nm excitation under dilute conditions. [c] Can be photoaggregated up to the Na_4 stage by 570-nm excitation of concentrated Na/Kr matrices (see Figure 4). [d] Suspected site splitting. [e] Small (roughly 6–12 nm) concentration-dependent shifts observed on these bands. [f] Photoaggregation, metal concentration, and bulk annealing suggest that this shoulder could be an Na_4 band. [g] A third possible site for sodium atoms absorbs at 500 nm;[39] seen as a shoulder on the 476–483-nm absorption of Na_2 in concentrated Na/Kr matrices and is found to be photointerconvertible with the blue sodium atom site from dilute Na/Kr experiments (see Figure 5). [h] From high Na/Kr = $1/10^3$ to $1/10^2$ concentration experiments (Figures 1, 4). It would appear that a higher Na_n cluster ($n \geq 4$) also absorbs in this region.

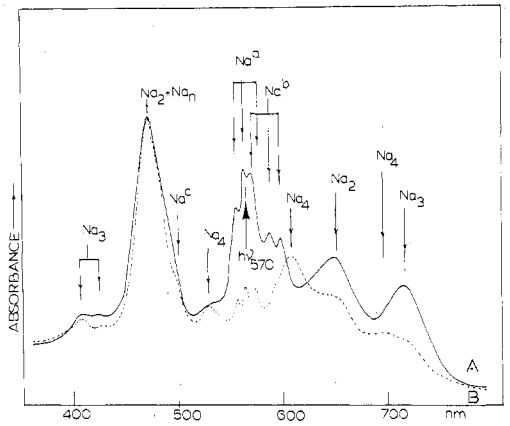

Figure 4. The effects (B) of 10 min of 570-nm narrow-band (8 nm) photoexcitation (xenon lamp, 600-W, Schoeffel monochromator assembly) into the sodium atom resonance absorptions of a $Na_{1,2,3,4}$/Kr matrix (A), pointing toward an efficient photoaggregation process of Na atoms to, at least, the Na_4 cluster stage (see text and ref 7 and 19).

around 698 nm with the intense Na_2, Na_3 absorptions near 657, 724 nm, respectively; these new cluster absorptions seem to display the growth behavior expected for the tetranuclear Na_4[42] stage, although overlap complications preclude a definite assignment (Figure 1, Table II).

At this stage of the discussion we wish to emphasize a remarkable resemblance between the optical spectra of $Na_{1,2,3,4}$ and $Ag_{1,2,3,4}$ in, for example, Kr matrices, not in the sense of absolute transition energies but rather in terms of the spectral distribution and intensities of the $M_{2,3,4}$ cluster absorptions straddling the $^2S_{1/2} \rightarrow {}^2P_{1/2,3/2}$ parent atomic resonance lines (illustrated in Figure 6). We believe that this is not a purely

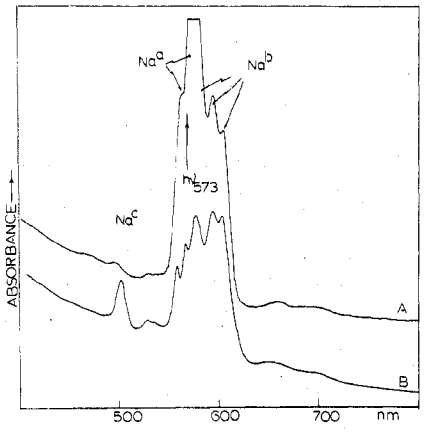

Figure 5. The matrix optical spectrum of an extremely dilute Na/Kr $\simeq 1/10^5$ matrix deposited at 10–12 K, showing (A) almost spectroscopically pure sodium atoms (Na^a and Na^b sites), followed by 573-nm photoconversion of the Na^a site to a new Na^c site, absorbing near 500 nm. Note that the Na^c site can be *partially* back-converted to the Na^a site by 500-nm photoexcitation and that the Na^a and Na^b sites are also interconvertible to some extent, as seen by sequential 560 nm/590 nm photoexcitation, respectively. (Such an effect has been referred to previously as optical pumping—see ref 39.)

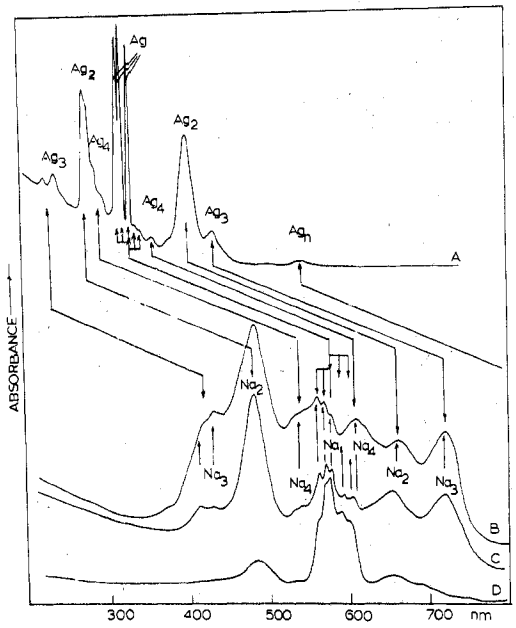

Figure 6. (A) The matrix optical spectra of $Ag_{1,2,3,4}$/Kr compared with (B)–(D) the matrix optical spectra of $Na_{1,2,3,4}$/Kr, recorded at 10–12 K.

serendipitous event but instead a prerequisite of the ns^1 isovalence of Na and Ag, the predominance of *n*s orbital contributions to the metal–metal bonding interactions, the uninvolvement of low-lying Ag 4d orbitals in the silver–silver bonding, the absence of Na 3d character in the sodium–sodium bond, and the mainly 3s → 3p and 5s → 5p localized character of the *visible* absorptions of $Na_{1,2,3,4}$ and *ultraviolet–visible* absorptions of $Ag_{1,2,3,4}$, respectively. The *blue* shifting of the $Ag_{1,2,3,4}$ excitation energies with respect to $Na_{1,2,3,4}$ is presumably an electronic manifestation of the more favorable 5s–5s overlap properties and the larger 5s/5p energy separations for atomic Ag compared to the 3s/3p of atomic Na.

The optical transition energies tentatively ascribed to Na_3 in the present study, like the corresponding ESR measurements,[18] clearly support the contention that Na_3 is a chemically real, bound species and not merely a three-atom van der Waals adduct. The ESR picture for Na_3[18] is one in which the unpaired electron has predominantly 3s character, lies in a weakly antibonding σ orbital, and has 93% of its spin density equally distributed between *two* of the sodium atoms, with only 7% spin density on the third.[18] The ESR spectra do not, however, present a clear-cut distinction between linear or nonlinear geometries for Na_3; moreover, a charge-separated $Na_2^+Na^-$ contributor could not be entirely ruled out.[18] Significantly, an ab initio configuration interaction study of the potential energy surface of Na_3[23] has recently predicted a ground state having an obtuse triangle $^2B_2$ symmetry and bound by only 8.5 kcal/mol relative to $Na_2(^1\sum_g^+)$ + $Na(^2S)$. The surface was found to be extremely flat, with two saddle points, an acute triangle ($^2A_1$ state) and a linear symmetric conformation ($^2\sum_u^+$ state) lying only 0.6 and 3.0 kcal/mol, respectively, above the minimum.[23] The theoretical suggestion for Na_3 is that of an easily deformable molecule, that is, an extremely "floppy molecule" with the entire chemically interesting portion of the computed potential energy surface lying within a 3-kcal range;[23] one must therefore be aware of the possibility of immobilizing more than a single structural form of Na_3 in "nonequilibrium", quench-condensed inert gas films containing Na_3.[46] In this context we note that the first reported matrix Raman data for Ag_3[11] showed a single intense breathing mode at 120 cm^{-1}, suggesting a linear geometry for Ag_3, consistent with earlier EHMO[44] and CNDO[44] calculations for Ag_3; however, a small distortion from linearity could have passed unnoticed in the reported Raman spectrum of Ag_3,[11] as well as unsuspected laser photoaggregation, resonance Raman/laser-induced fluorescence, and impurity complications.[11] In this same vein, recent ESR observations for argon-entrapped, photogenerated Ag_3[19] showed large, hyperfine coupling of the unpaired electron to *two equivalent silver atoms* (with superimposed $^{107}Ag/^{109}Ag$ confirmatory isotopic splittings), consistent with the idea of a mainly 5s localized electron in either a linear or bent Ag_3 molecule.

Although our optical data for Na_3 cannot be considered as being definitive in a structural sense, it is nevertheless instructive to compare the data with the most intense optical excitations predicted for the obtuse, triangular $^2B_2$ ground state of Na_3, by recent ab initio configuration interaction computational techniques.[23] In essence, at least 13 spin- and dipole-allowed 3s → 3p localized transitions are calculated to occur in the visible range of Na_3, considerably in excess of that observed experimentally.[23] These excitations are, however, predicted to have quite disparate oscillator strengths and, moreover, their associated energies fall within two main groups centered around 600 and 400 nm.[23] Taking into account the substantial band widths of the 720–750/405–426 nm visible absorptions of Na_3 in Kr and Xe matrices, one is tempted to conclude that experiment and theory agree quite well for an assumed obtuse, triangular Na_3 geometry. Clearly, for linear Na_3, fewer dipole-allowed transitions would be expected in the visible range. However, transition-state energy calculations are as yet unavailable for linear Na_3 and a meaningful distinction between geometrical isomers of Na_3 cannot presently be achieved. Similar reasoning is likely to hold true for linear vs. nonlinear Ag_3.

A final word regarding the tetranuclear clusters is probably in order. Even less is known about this intriguing class of molecular aggregates than was mentioned for the M_3 types. We note that preliminary Raman studies[11] of heavily doped Ag/Kr matrices appear to display a single ν(AgAg) stretching mode which might be ascribed to Ag_4. A high-symmetry T_d structure for Ag_4 would be consistent with this preliminary Raman observation, rather than the EHMO/CNDO favored model of linearity for Ag_4.[44]

Although a linear structure was not considered in some recent SCF–Xα–SW calculations for Li_4,[45] the Xα statistical total energy slightly favored a tetrahedral geometry over that

for square-planar Li_4. However, a Jahn–Teller distortion of the Li_4 tetrahedron to a lower symmetry such as C_{3v} would have the effect of lowering the total energy, although SCF–Xα–SW calculations have not yet been reported on the C_{3v} form to determine the energy differential. Presumably, the optical data of the present study for Na_4, when taken in conjunction with further IR/Raman observations and ab initio CI calculations for Na_4, will help toward clarifying the electronic and geometric properties of this fascinating tetranuclear metallic molecule.

Acknowledgment. We wish to acknowledge extremely helpful discussions with Dr. W. Schulze and his co-workers at the Fritz Haber Max-Planck Institute, West Berlin, concerning our sodium cluster experimental results and express our appreciation to Dr. E. Schumacher and his co-workers at the University of Berne, Berne, Switzerland, and Dr. T. Welker and his co-workers at the Max-Planck Institut Physikalische Chemie, Technische Hochschule, Darmstadt, West Germany, for bringing to our attention some of their theoretical and experimental studies with alkali metal clusters. The financial assistance of the National Research Council of Canada New Ideas, Strategic Energy and Operating Grant Programmes, Imperial Oil of Canada, Atkinson Foundation, Connaught Fund, Lash Miller Chemical Laboratories, and Erindale College is all gratefully acknowledged.

Registry No. Na, 7440-23-5; Na_2, 25681-79-2; Na_3, 37279-42-8; Na_4, 39297-86-4.

References and Notes

(1) R. P. Messmer, S. K. Knudson, K. H. Johnson, J. B. Diamond, and C. Y. Yang, *Phys. Rev. B*, **13**, 1396 (1976), and references cited therein.
(2) G. A. Ozin, *Cat. Rev. Sci. Eng.*, **16**, 191 (1977), and references cited therein.
(3) R. P. Messmer in "The Nature of the Chemisorption Bond", G. Ertl and T. Rhodin, Eds., North-Holland Publishing Co., Amsterdam, 1978, and references cited therein.
(4) G. A. Ozin and W. E. Klotzbücher, *J. Mol. Catal.*, **3**, 195 (1977); *J. Am. Chem. Soc.*, **100**, 2262 (1978).
(5) J. Hulse and M. Moskovits, *J. Chem. Phys.*, **66**, 3988 (1977).
(6) (a) J. Hulse and M. Moskovits, *J. Chem. Phys.*, **67**, 4271 (1977); (b) L. Noodleman, J. G. Norman, Jr., G. A. Ozin, and S. Mitchell, *J. Am. Chem. Soc.*, in press.
(7) G. A. Ozin and H. Huber, *Inorg. Chem.*, **17**, 155 (1978); W. Schulze, H. U. Becker, and H. Abe, *Ber. Bunsenges. Phys. Chem.*, **82**, 7 (1978).
(8) (a) P. A. Montano, *J. Appl. Phys.*, **49**, 1561 (1978); (b) *J. Am. Chem. Soc.*, in press.
(9) A. Bos and A. T. Howe, *J. Chem. Soc., Faraday Trans. 2*, **70**, 440, 451 (1974).
(10) P. Barrett and P. Montano, *Ber. Bunsenges. Phys. Chem.*, **82**, 30 (1978); *J. Chem. Soc., Faraday Trans. 2*, **73**, 378 (1977).
(11) W. Schulze, H. U. Becker, R. Minkwitz, and K. Marzel, *Chem. Phys. Lett.*, **55**, 59 (1978), and private communication.
(12) A. Givan and A. Loewenschuss, *J. Chem. Phys.*, **69**, 1790 (1978).
(13) V. F. Bondybey and J. H. English, *J. Chem. Phys.*, in press.
(14) V. E. Bondybey, private communication.
(15) V. E. Bondybey and J. H. English, *J. Chem. Phys.*, **67**, 3405 (1977).
(16) G. Kenney-Wallace, G. A. Ozin, S. Mitchell, and J. Farrel, paper first presented by G. A. Ozin at the cluster Symposium, Materials Research Society, Boston, June 1978 (to be submitted for publication).
(17) P. H. Kasai and D. McLeod, Jr., *J. Phys. Chem.*, **82**, 1554 (1978).
(18) D. M. Lindsay, D. R. Herschbach and A. L. Kwiram, *Mol. Phys.*, **32**, 1199 (1976), and references cited therein.
(19) G. A. Ozin and H. Huber, unpublished work.
(20) T. H. Upton and W. A. G. Goddard, III, *J. Am. Chem. Soc.*, **100**, 5659 (1978); J. Kendrick and I. H. Hillier, *Mol. Phys.*, **33**, 635 (1977); P. S. Bagus, G. del Conde, and D. W. Davies, *Faraday Discuss. Chem. Soc.*, **62**, 321 (1977), and references cited therein.
(21) (a) P. J. Foster, R. E. Leckenby, and E. J. Robbins, *J. Phys. B*, **2**, 478 (1969); (b) R. J. Gordon, Y. T. Lee, and D. R. Herschbach, *J. Chem. Phys.*, **54**, 2393 (1971); A. Herrmann, E. Schumacher, and L. Wöste, *ibid.*, **68**, 2327 (1978); A. Hermann, S. Leutwyler, E. Schumacher, and L. Wöste, *Helv. Chim. Acta*, **61**, 453 (1978); *Chem. Phys. Lett.*, **52**, 418 (1977), and references cited therein.
(22) K. Kimoto and I. Nishida, *J. Phys. Soc. Jpn.*, **42**, 2071 (1977).
(23) R. L. Martin and E. R. Davidson, private communication.
(24) G. A. Ozin and H. Huber, unpublished work.
(25) M. Moskovits and G. A. Ozin, *J. Appl. Spectrosc.*, **26**, 481 (1972); E. P. Kündig, M. Moskovits, and G. A. Ozin, *J. Mol. Struct.*, **14**, 137 (1972).
(26) L. Andrews and G. C. Pimentel, *J. Chem. Phys.*, **47**, 2905 (1967); B. Meyer, *J. Chem. Phys.*, **43**, 2986 (1965); W. Weyhmann and F. M. Pipkin, *Phys. Rev.*, **137**, A490 (1964); R. B. Merrithew, G. V. Marusak, and C. E. Blount, *J. Mol. Spectrosc.*, **29**, 54 (1969); W. R. M. Graham and W. W. Duley, *J. Chem. Phys.*, **55**, 2527 (1971); J. D. McCullough and W. W. Duley, *Chem. Phys. Lett.*, **15**, 240 (1972), and references cited therein.
(27) D. M. Gruen in "Cryochemistry", M. Moskovits and G. A. Ozin, Ed., Wiley, New York, 1976.
(28) Von. B. Mile, *Angew. Chem., Int. Ed. Engl.*, **7**, 507 (1968).
(29) F. K. Chi and L. Andrews, *J. Phys. Chem.*, **77**, 3062 (1973); L. Andrews and J. I. Raymond, *J. Chem. Phys.*, **55**, 3087, 1971.
(30) L. Andrews and R. C. Spiker, Jr., *J. Phys. Chem.*, **76**, 3208 (1972).
(31) J. J. Turner and P. A. Breeze, *J. Organomet. Chem.*, **44**, C7 (1972).
(32) P. H. Kasai, *Acc. Chem. Res.*, **4**, 329 (1971), and references cited therein.
(33) R. G. Doerr and P. S. Skell, *J. Am. Chem. Soc.*, **89**, 3062 (1967).
(34) M. Andrews, J. Guillet, and G. A. Ozin, unpublished work.
(35) P. Timms and B. Scott, private communication; P. N. Hawker, E. P. Kündig, and P. L. Timms, *J. Chem. Soc., Chem. Commun.*, 730 (1978). Note that in ref 27–35 we focus our attention on sodium atoms for studying multiple trapping site effects and matrix-induced frequency shifts,[27] as a halogen abstraction agent for generating and studying a wide range of organic (e.g., $Na + CH_2ClCH{=}CHCH_3 \rightarrow \cdot CH_2CH{=}CHCH_3 + NaCl$[28]) and inorganic (e.g., $Na + OCl_2 \rightarrow NaCl + OCl$[29]) free radicals, as an electron transfer agent (e.g., $Na + O_3 \rightarrow Na^+O_3^-$) for producing a variety of molecular ion pairs,[30] and as a photoelectron source (e.g., $Na + Cr(CO)_6/Ar \rightarrow Na^+[Cr(CO)_5^-]$,[31] $Na + B_2H_6/Ar \rightarrow Na^+[B_2H_6^-]$,[32] $Na + Ag/Xe \rightarrow Na^+[Ag^-]$[24]) for creating novel anionic atomic and molecular species. Furthermore, Na (and K) atom reactions have been used in organic synthesis, e.g.

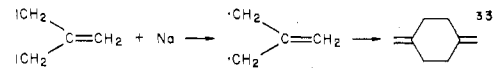

[33]

and for anionic-initiated, solid-state cryopolymerizations, e.g.

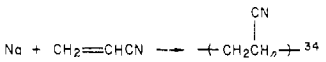

[34]

as well as for the generation of active metals for organometallic synthesis (e.g., $K + \text{arene} + MX_2 \rightarrow KX + (\text{arene})_2M$[35]).
(36) D. Nagel and B. Sonntag, *Ber. Bunsenges. Phys. Chem.*, **82**, 38 (1978).
(37) W. R. M. Graham and W. W. Duley, *J. Chem. Phys.*, **54**, 586 (1971).
(38) L. Andrews, *J. Mol. Spectrosc.*, **61**, 337 (1976).
(39) L. C. Balling, M. D. Havey, and J. F. Dawson, *J. Chem. Phys.*, **69**, 1670 (1978).
(40) M. Moskovits and G. A. Ozin in "Cryochemistry", M. Moskovits and G. A. Ozin, Ed., Wiley, New York, and references cited therein.
(41) S. W. Charles and G. C. Pimentel, *Pure Appl. Chem.*, **7**, 111 (1963).
(42) M. Moskovits and J. Hulse, *J. Chem. Soc., Faraday Trans. 2*, 471 (1977).
(43) G. Hertzberg in "Spectra of Diatomic Molecules", D. Van Nostrand, New York, 1970.
(44) R. C. Baetzold, *J. Catal.*, **29**, (1979); *J. Chem. Phys.*, **55**, 4355, 4363 (1971); *J. Phys. (Paris)* C2, 175 (1975), and references cited therein.
(45) J. G. Fripiat, K. T. Chow, M. Boudart, J. B. Diamond, and K. H. Johnson, *J. Mol. Catal.*, **1**, 59 (1975/76).
(46) Of significance here are the results of an ab initio calculation of the Born–Oppenheimer potential energy hypersurface and lowest vibronic states of Li_3 which emphasize the high probability of finding the Li_3 molecule in any one of three equivalent obtuse angled isosceles triangular forms. For an unrestricted gaseous Li_3 molecule this would lead to a time-averaged fluxional D_{3h} geometry. A static Jahn–Teller distortion of Li_3 (or Na_3, with its anticipated softer deformational and stretching modes) requires that the lowest vibronic state be well localized in any one of three equivalent distorted geometries. It is likely that Li_3 (Na_3 or Ag_3) immobilized in the rigid cage environment of a low-temperature inert gas matrix (or Ag_3 on the surface of, or within the lattice confines of a room temperature oxide support) could be "clamped" in an obtuse angled isoscles triangular form (taken from W. H. Gerber and E. Schumacher, preprint and *J. Chem. Phys.*, in press).